



## IL-1 $\beta$ stimulates a novel axis within the NF $\kappa$ B pathway in endothelial cells regulated by IKK $\alpha$ and TAK-1

Rachel Craig<sup>1</sup>, Kathryn McIntosh<sup>\*</sup>, Ka Ho Ho, Ashley McCulloch, Christopher Riley, Christopher Lawson, Simon P. Mackay, Andrew Paul, Paul Coats, Robin Plevin<sup>\*</sup>

Strathclyde Institute for Pharmacy and Biomedical Sciences, University of Strathclyde, 161 Cathedral Street, Glasgow, G4 0RE, Scotland, UK

### ARTICLE INFO

#### Keywords:

NF $\kappa$ B  
IL-1 $\beta$   
Signalling  
IKK $\alpha$   
TAK-1  
HUVECs

### ABSTRACT

In this study we examined the activation of the non-canonical NF $\kappa$ B signalling pathway in endothelial cells. In HUVECs, LIGHT stimulated a delayed induction of serine 866/870 p100 phosphorylation linked to p52 NF $\kappa$ B formation. Surprisingly, the canonical ligand, IL-1 $\beta$ , stimulated a rapid phosphorylation of p100 which was not associated with p52 formation. Inhibition of IKK $\alpha$  activity, using DN-IKK $\alpha$  adenovirus, IKK $\alpha$  siRNA or a novel first-in-class selective IKK $\alpha$  inhibitor, SU1261, revealed IL-1 $\beta$  induced p100 phosphorylation to be dependent on IKK $\alpha$ . In contrast, IKK $\beta$  inhibition was found to be without effect. The NIK inhibitor, CW15337, did not affect IL-1 $\beta$  induced p100 phosphorylation however, both p100 and pIKK $\alpha$ / $\beta$  phosphorylation was substantially reduced by inhibition of the upstream kinase TAK-1, suggesting phosphorylation of p100 is mediated by IKK $\alpha$  from within the canonical NEMO/IKK $\beta$ /IKK $\alpha$  complex. IL-1 $\beta$  also stimulated a rapid increase in nuclear translocation of p52, which was not affected by NIK inhibition, suggesting a source of p52 independent of p100 processing. Inhibition of TAK-1 abolished p52 and p65 nuclear translocation in response to IL-1 $\beta$ . siRNA deletion or inhibition with dominant-negative virus of IKK $\alpha$  activity partially reduced p52 translocation, however pharmacological inhibition of IKK $\alpha$  was without effect. Inhibition of IKK $\beta$  abolished both p52 and p65 translocation. Taken together these results show that IL-1 $\beta$  stimulates a novel IKK $\alpha$ -dependent axis within the non-canonical NF $\kappa$ B pathway in endothelial cells which is NIK-independent and regulated by TAK-1. However, this pathway is not primarily responsible for the early nuclear translocation of p52, which is dependent on IKK $\beta$ . Elucidation of both these new pathways may be significant for NF $\kappa$ B biology within the endothelium.

### 1. Introduction

The nuclear factor Kappa B cascade is a major multi-component transcription factor pathway which plays a key role in normal physiology and diseases including; arthritis, cancer, cardiovascular disease and CNS disorders [1]. The cascade has two major components; the classical or canonical pathway and the non-canonical pathway [2]. Both these pathways are regulated through a multi-kinase complex known as inhibitory kappa B kinase (IKK) comprising of the active intermediates, IKK $\alpha$  and  $\beta$ , and additionally IKK $\gamma$  or NEMO which is specifically part of the canonical pathway.

For activation of the canonical pathway mediated by ligands such as TNF $\alpha$  and IL-1 $\beta$  regulation is focussed on the NEMO/IKK $\alpha$ /IKK $\beta$  complex. Within this complex, IKK $\beta$  phosphorylates I $\kappa$ B $\alpha$ , liberating p65 NF $\kappa$ B, which translocates to the nucleus to regulate gene function. In comparison non-canonical NF $\kappa$ B signalling (see reviews by [3,4]) is activated by ligands such as CD40, lymphotoxin alpha1/beta2 (LT $\alpha$ 1 $\beta$ 2) and LIGHT ligand [5]. Upon activation NF $\kappa$ B inducing-kinase (NIK) drives the activation of IKK $\alpha$  homodimers which promotes the phosphorylation and degradation of a large I $\kappa$ B, p100 NF $\kappa$ B2 unit, liberating the NF $\kappa$ B isoform, p52. NIK is also critically involved in the degradation/processing of p100 by inducing the binding of p100 to the beta-

**Abbreviations:** NF $\kappa$ B, Nuclear factor kappa B; IL-1 $\beta$ , Interleukin 1 beta; TNF $\alpha$ , Tumour-necrosis factor-alpha; LIGHT, homologous to lymphotoxin, exhibits inducible expression and competes with HSV glycoprotein D for binding to herpesvirus entry mediator, a receptor expressed on T lymphocytes; IKK $\alpha$ , Inhibitory Kappa B Kinase  $\alpha$ ; IKK $\beta$ , Inhibitory Kappa B Kinase  $\beta$ ; NEMO, NF- $\kappa$ B essential modulator; TAK-1, transforming growth factor beta-activated kinase 1; NIK, NF-kappa-B-inducing kinase.

<sup>\*</sup> Corresponding authors.

E-mail addresses: [kathryn.a.mcintosh@strath.ac.uk](mailto:kathryn.a.mcintosh@strath.ac.uk) (K. McIntosh), [r.plevin@strath.ac.uk](mailto:r.plevin@strath.ac.uk) (R. Plevin).

<sup>1</sup> Current Address: Paul O'Gorman Leukaemia Research Centre, Institute of Cancer Sciences, University of Glasgow, Glasgow, UK

<https://doi.org/10.1016/j.bcp.2024.116736>

Received 27 August 2024; Received in revised form 11 December 2024; Accepted 19 December 2024

Available online 20 December 2024

0006-2952/© 2024 The Authors. Published by Elsevier Inc. This is an open access article under the CC BY license (<http://creativecommons.org/licenses/by/4.0/>).

transducin repeats-containing proteins ( $\beta$ -TrCP) E3 ubiquitin ligase [6–8]. However, in resting cells the levels of NIK are very low; the protein is continually targeted to the proteasome via TRAF3 [9] and TRAF2/cIAP1/2 [10,11]. Thus, activation of this pathway is characteristically slow, and dependent on the release of NIK from proteasomal degradation and associated with the formation of cellular p52 and the processing of p100 [3,4].

Assessment of the non-canonical NF $\kappa$ B pathway in cells of the cardiovascular system such as endothelial cells has been limited relative to other cell types. Original studies [12] identified a role for IKK $\alpha$  in LIGHT and lymphotoxin-mediated induction of CXCL12, whilst other work characterised the stimulation of noncanonical NF $\kappa$ B signalling in response to CD40 ligand [13] or RANKL [14]. A more recent study has linked NIK to both IKK $\alpha$  and IKK $\beta$  with respect to endothelial cell inflammatory gene expression in response to lymphotoxin stimulation [15] suggesting an interaction between the two pathways. Furthermore, it has also been shown that activation of the canonical NF $\kappa$ B pathway by TNF $\alpha$  inhibits the corresponding noncanonical pathway in endothelial cells [16] and indeed this a well-recognised cross regulatory effect between the pathways [17]. Such studies give insight into the feasibility of selectively targeting either NF $\kappa$ B pathway to realise potential therapeutic benefits. [18].

Having previously discovered a novel role for IL-1 $\beta$  mediated non-canonical signalling in a cancer cell setting, we sought to examine the regulatory effects of IL-1 $\beta$  in a non-disease system looking at primary cardiovascular cells. We found that IL-1 $\beta$  in this setting was also able to stimulate a strong early activation of p100 NF $\kappa$ B2 phosphorylation, an event that is normally linked to non-canonical pathway activation. This novel event was found to be IKK $\alpha$  dependent but NIK independent and interestingly sensitive to TAK-1 inhibition suggesting that IKK $\alpha$  functions as part of the NEMO/IKK $\alpha$ /IKK $\beta$  complex. We also demonstrate a rapid nuclear translocation of p52 in response to IL-1 $\beta$ , partially dependent on IKK $\alpha$  activation but wholly reliant on canonical NF $\kappa$ B signalling via IKK $\beta$ . These findings reveal a novel paradigm with respect to the activation of elements of the non-canonical NF $\kappa$ B pathway by canonical pathway ligands in endothelial cells.

## 2. Materials and methods

### 2.1. Reagents

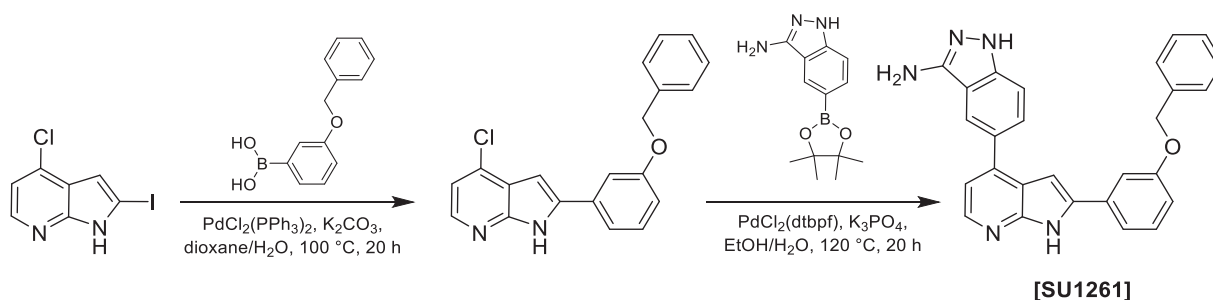
All reagents were from the highest quality commercial sources Sigma-Merck (Poole, UK), unless otherwise stated. Antibodies were

manufactured by Dharmacon and purchased from Horizon discovery ltd (Cambridge, UK). The agonists used for stimulation were purchased as follows, both Human recombinant TNF $\alpha$  and IL-1 $\beta$  from Insight Biotechnology (Wembley, UK) and Human recombinant Lymphotoxin  $\alpha$ 1 $\beta$ 2 and LIGHT from R&D systems (McKinley Place NE, Minneapolis).

The NIK inhibitor, CW15337, was synthesised in house as outlined previously [19].

### 2.2. Synthesis of SU1261 [5-(2-(3-(benzyloxy)phenyl)-1H-pyrrolo[2,3-b]pyridin-4-yl)-1H-indazol-3-amine]

All commercially available reagents and solvents used were obtained from Merck, Fluorochem, Fisher Scientific, Acros, Alfa Aesar, and Apollo scientific and used without further purification. Air- sensitive reactions were carried out under an argon or nitrogen atmosphere. All compounds were determined to be  $\geq 95$  % purity by LC-MS and analytical HPLC unless otherwise stated. Flash chromatography was performed using a Biotage SP4 automated chromatography system using silica stationary phase (Fisher Scientific, 60  $\text{\AA}$ , 35–70  $\mu\text{m}$ ; detection wavelength: 254 nm; monitoring: 280 nm) and the mobile phase used are detailed in the text. Reverse phase HPLC purifications were conducted on Shimadzu Prominace HPLC using a semi-preparative (50 x 21.2 mm) Luna 5  $\mu\text{m}$  C18 column at 40  $^{\circ}\text{C}$ ; flow rate: 6 ml/min; detection wavelength: 254 nm eluting with an acetonitrile/water gradient with 0.1 % TFA. NMR spectra were recorded on either a Bruker Avance3/DPX400 (400 MHz), Bruker DRX500 (500 MHz), Bruker AV400 (400 MHz), Bruker AV500HD (500 MHz) or Bruker AV600 (600 MHz) instrument and analysed using Advanced Chemistry Development Labs (ACD/labs) NMR processor 12.00 or MestReNova 10.0 software. Chemical shifts ( $\delta$ ) are recorded in parts per million (ppm) relative to an internal solvent reference (tetramethylsilane) and coupling constants ( $J$ ) in Hertz (Hz). Splitting patterns were indicated as singlet (s), broad singlet (br s), doublet (d), doublet of doublet (dd), triplet (t), quartet (q) and multiplet (m). LC-MS was carried out on an Agilent Technologies 1220 series LC system with Agilent 6100 series quadrupole mass spectrometer in ESI/APCI mode. Separation was achieved with an Agilent Eclipse C18 4.6x50 mm column; flow rate: 1 mL/min; detection: 254 nm; sample volume: 10  $\mu\text{l}$ ; mobile phase: acetonitrile/ 5 mM ammonium acetate: water/5mM ammonium acetate; 5 %, 1.48 min; 5–100 %, 8 min; 100 %, 13.5 min; 100–5 %, 16.5 min; 18 min. HRMS was carried out on an Exactive (Thermo scientific) or LTQ orbitrap (Thermo scientific).



purchased as follows: pp100 (serine 866/870), p100/p52, ppIKK $\alpha$ / $\beta$ , pp65, ppJNK, pJNK, NF $\kappa$ B, I $\kappa$ B $\alpha$ , nucleolin and GAPDH from Cell Signalling technology (Europe); IKK $\alpha$  was purchased from Merck-Millipore (UK) and IKK $\beta$  from Abcam ltd (Cambridge, UK). HRP-conjugated secondary antibodies manufactured by Jackson Immuno Research laboratories Inc. (West Grove, PA, USA) and purchased from Stratech Scientific (Ely, UK). IKK2-XI inhibitor was from Calbiochem (CAS 354810–80-3) and purchased through Sigma-Merck (Poole UK). IKK $\alpha$  siRNA was

In step 1, a suspension of 4-chloro-2-iodo-7-azaindole (0.343 g, 1.23 mmol), 3-(benzyloxy)phenylboronic acid (0.348 g, 1.52 mmol), K<sub>2</sub>CO<sub>3</sub> (0.483 g, 3.49 mmol) and bis(triphenylphosphine) palladium(II) chloride (0.074 g, 0.105 mmol) in dioxane (3 mL) and water (2 mL) was degassed under nitrogen. The reaction mixture was allowed to stir at 100  $^{\circ}\text{C}$  for 20 h, then cooled to room temperature and extracted between ethyl acetate (5 mL) and water (3 mL). The organic layer wash washed

with brine (2 × 3 mL), dried over anhydrous sodium sulfate and concentrated under reduced pressure. The crude residue was used in the next step without further purification.

In step 2, a solution of K<sub>3</sub>PO<sub>4</sub> (1 M, 1.2 mL) was added to a suspension of (3-(benzyloxy)phenyl)-4-chloro-1*H*-pyrrolo[2,3-*b*]pyridine (0.124 g, 0.37 mmol), 5-(4,4,5,5-tetramethyl-1,3,2-dioxaborolan-2-yl)-1*H*-indazol-3-amine (0.146 g, 0.56 mmol) and [1,1'-bis(di-*tert*-butylphosphino)ferrocene]dichloro palladium(II) catalyst (0.028 g, 0.04 mmol) in ethanol (3 mL) and water (2 mL). The reaction mixture was heated to 120 °C for 20 h, then cooled to room temperature, diluted with ethyl acetate and washed with water and brine. The organic layer was dried over anhydrous sodium sulfate and concentrated under reduced pressure. The crude residue was purified by column chromatography (90 % ethyl acetate in petroleum ether) to afford SU1261 as an off-white solid (0.092 g, 58 %). <sup>1</sup>H NMR (500 MHz, DMSO-*d*<sub>6</sub>) δ 12.21 (s, 1H), 11.56 (s, 1H), 8.27 (d, *J* = 5.0 Hz, 1H), 8.25 (s, 1H), 7.73 (d, *J* = 8.4 Hz, 1H), 7.69 (s, 1H), 7.59 (d, *J* = 7.6 Hz, 1H), 7.51 (d, *J* = 7.6 Hz, 2H), 7.43–7.39 (m, 4H), 7.38–7.32 (m, 2H), 7.23–7.19 (m, 2H), 6.99 (d, *J* = 8.4 Hz, 1H), 5.55 (s, 2H), 5.21 (s, 2H). <sup>13</sup>C NMR (126 MHz, DMSO-*d*<sub>6</sub>) δ 158.85, 150.43, 149.89, 143.32, 141.19, 141.08, 138.05, 137.04, 133.00, 129.96, 128.44, 127.87, 127.82, 127.70, 126.69, 120.35, 118.40, 118.06, 114.62, 114.50, 114.46, 111.62, 109.95, 97.28, 69.36. HRMS (ESI): exact mass calculated for C<sub>27</sub>H<sub>21</sub>N<sub>5</sub>O: 431.1746, found 432.1817 (M + 1)<sup>+</sup>.

### 2.3. Synthesis of CW15337

The NIK inhibitor CW15337 was synthesised as outlined previously [19].

### 2.4. Cell culture

Cryopreserved primary HUVECs (from pooled donors) and media were purchased from Lonza (Slough, UK), and grown in endothelial basal media (EBM-2). Media was supplemented with single aliquots of defined supplements (2 % foetal bovine serum, 0.2 mL hydrocortisone, 2 mL rh fibroblast growth factor-B, 0.5 mL vascular endothelial growth factor, 0.5 mL R3-insulin-like growthfactor-1, 0.5 mL ascorbic acid, 0.5 mL rh epidermal growth factor, 0.5 mL GA-1000 and 0.5 mL heparin (concentrations not disclosed by the company)). Cells were incubated at 37 °C in humidified air with 5 % CO<sub>2</sub>; medium was changed every 2 days thereafter until cells became confluent and passaged in 1 % trypsin/EDTA solution. All experiments were performed between passages 2 and 6, in either 6 or 12-well plates.

### 2.5. Western Blot analysis

Whole cell lysates were prepared from HUVECs and the status of phosphorylated and total proteins assessed by Western blotting as described previously [20]. Briefly cells were stimulated with agonist for the indicated times in complete medium. Proteins (approximately 15 µg) were separated by either 8.5 or 10 % SDS-PAGE and transferred onto nitro-cellulose. The membranes were blocked for non-specific binding for 2 h in 2 % BSA (w/v) diluted in NATT buffer (20 mM Tris, 150 mM NaCl, 0.2 % (v/v) Tween-20, pH 7.4). Membranes were then incubated overnight with primary antibody diluted in 0.2 % BSA (w/v) in NATT buffer at 4 °C with rotation. The membranes were then washed with NATT buffer for 90 min (6 × 15 min) and incubated with horseradish peroxidase (HRP)-conjugated secondary antibody for 2 h. After a further 60 min wash (4 × 15 min), the membranes were subjected to ECL reagent and exposed to Kodak X-ray film for appropriate time (Kodak, Amsterdam, Netherlands).

### 2.6. Nuclear extracts

Confluent cells grown on 6-well plates, were incubated with LIGHT

or IL-1β under experimental conditions as indicated. Following washing in ice cold PBS, cells were scraped into PBS and centrifuged at 13,000g for 1 min at 4 °C. Pellets were resuspended in 200 µl buffer 1 (10 mM HEPES, 10 mM KCl, 0.1 mM EDTA, 0.1 mM EGTA, 0.5 mM PMSF, 1 µg/ml aprotinin, 1 µg/ml leupeptin, 10 µg/ml pepstatin pH 7.9) and incubated on ice for 15 min. After addition of 25 µl 10 % (w/v) NP-40 samples were vortexed and centrifuged at 13,000g for 2 min. Pellets were re-suspended in 50 µl buffer 2 (20 mM HEPES, 25 % (v/v) Glycerol, 0.4 M NaCl, 1 mM EDTA, 1 mM EGTA, 0.5 mM PMSF, 1 µg/ml Aprotinin, 1 µg/ml Leupeptin, 1 µg/ml pepstatin pH 7.9) and vortexed briefly before shaking (IkA-Vibrax-vxr) at 4 °C for 15 min. Samples were then sonicated (Ultrawave U50) on ice for 1 min and centrifuged at 13,000g for 15 min. Samples were equilibrated for protein content using a standard Bradford's reagent before Western blotting.

### 2.7. Adenovirus infection

Adenoviral vectors encoding dominant-negative IκB kinase alpha or beta (Adv.DN-IKKα and β) were purified in-house using the Adeno-X virus purification kit from Clontech Laboratories, Inc. (Mountain View, CA, USA) [21]. The DN-IKKα and β plasmids was originally a gift from Dr D.Goeddel (Tularik Inc., San Francisco, CA, USA). Large-scale production of high-titre recombinant adenovirus was performed in HEK293 cells by routine methods. HUVECs, when approximately 50–60 % confluent, were counted and M.O.I calculated relative to the concentration of the virus. Wells were then incubated with adenovirus concentrations ranging from 50 to 500 pfu/ml for 40 h in endothelial growth media.

### 2.8. siRNA silencing of IKKs

HUVECs were transfected with ON-TARGET plus siRNA (Dharmacon/Horizon – Cambridge, UK) against sequences for IKKα (Human CHUK, #J-003473–09) or ON-TARGET plus siRNA against sequences for IKKβ (Human IKKBK, #J-003503–13) and non-targeting sequence (NT) was used as a negative control (non-targeting #1, #D-001810–01–20). Fugene 4 K (Promega – Hampshire, UK) diluted in Endothelial basal media was used to deliver the siRNA to the cells over 72 h. After 18 h media was replaced with fresh EBM-2 and cells maintained to 72 hrs before stimulation.

### 2.9. Data analysis

Each figure represents one of at least 4 independent experiments, unless otherwise stated. Western blots were scanned on an Epson perfection 1640SU scanner using Adobe photoshop 5.0.2 software. For gels, densitometry measurement was performed using the Scion Image program. Data were normalised to fold expression, independent replicates averaged and expressed as mean ± s.e.m. Statistical analysis was performed by One-way ANOVA with Dunnett's Post-test (\**p* < 0.05, \*\**p* < 0.01, \*\*\**p* < 0.001, \*\*\*\**p* < 0.0001).

## 3. Results

Initially, we examined the kinetics of LIGHT induced 866/870 p100 phosphorylation, known to be a key early event in the activation of non-canonical signalling mediated by IKKα [4] (Fig. 1). LIGHT stimulated a well-recognised, delayed increase in pp100 (serine 866/870) which was apparent by 1 h and sustained for up to 24 h at 8-fold of basal values (Fold increase: LIGHT, 24hr = 8.724 ± 2.087, \**p* < 0.05) of basal values (Fig. 1, Panel A). This correlated with the cellular accumulation of p52 NFκB (p52) which was apparent by 2 h and sustained for up to 24 h. In contrast, we identified a far earlier kinetic profile for IL-1β (Fig. 1, Panel B); the phosphorylation of p100 was rapid and maximal at as early as 15 min at a comparable level of stimulation (Fold increase: IL-1β, 15 min = 7.277 ± 2.159, \**p* < 0.05), but was transient returning to basal values

within 2 h. There was no significant increase in cellular p52 accumulation across this time period.

Given the rapid activation of p100 phosphorylation by IL-1 $\beta$ , at residues known to be regulated by IKK $\alpha$ , we sought to determine if this event was indeed mediated by IKK $\alpha$  (Fig. 2). We initially used dominant-negative-Adv.IKK $\alpha$  as an approach; infection with 250 and 500 pfu of this virus caused a significant reduction in IL-1 $\beta$  induced p100 phosphorylation (Fold increase: IL-1 $\beta$  +  $\beta$ -gal =  $10.34 \pm 1.109$  vs. IL-1 $\beta$  + 500 DN-IKK $\alpha$  =  $2.265 \pm 0.275$ , \*\*\*\*P < 0.0001) (Fig. 2, panel A). As expected, LIGHT-induced pp100 was significantly reduced at both concentrations tested. We also utilised siRNA for IKK $\alpha$  (Fig. 2, Panel B), which also caused a significant reduction in IL-1 $\beta$  induced phosphorylation decreasing stimulated levels to approximately 20 % of initial values (Fold increase: N/T + IL-1 $\beta$  =  $10.2 \pm 0.578$  vs. IKK $\alpha$  siRNA + IL-1 $\beta$  =  $2.851 \pm 0.686$ , \*\*\*\*P < 0.0001).

It is recognised that knockdown of one element of the NEMO/IKK complex may affect overall activation due to disruption of the complex itself. Therefore, to clarify the specific role of IKK $\alpha$  further, we utilised a novel, first-in-class, selective IKK $\alpha$  inhibitor, SU1261, developed in-house via an IKK $\alpha$  inhibitor drug discovery programme at the University of Strathclyde. SU1261 has demonstrated selective IKK $\alpha$  inhibition over IKK $\beta$  (IKK $\alpha$   $K_i$  = 10 nM, IKK $\beta$   $K_i$  = 680 nM) using a cell-free dissociation enhanced ligand fluorescent immunoassay (DELFLIA) as described in [22]. This IKK-isoform selectivity was recapitulated in a metastatic prostate cancer cell line (PC3m) using LT $\alpha_1\beta_2$ -stimulated p100 phosphorylation as a pharmacodynamic marker for IKK $\alpha$  activity, (IC $_{50}$  = 0.57  $\mu$ M), without perturbing markers of the IKK $\beta$ -driven canonical NF- $\kappa$ B pathway, represented by TNF $\alpha$ -stimulated I $\kappa$ B $\alpha$

degradation or p65 (Ser536) phosphorylation, [23].

As shown in Fig. 3, pre-incubation of HUVECs with SU1261 caused a concentration dependent inhibition of IL-1 $\beta$  induced pp100 phosphorylation (Fold increase: IL-1 $\beta$  + DMSO =  $7.198 \pm 0.864$  vs. 3  $\mu$ M =  $2.594 \pm 0.125$ , \*\*\*P > 0.001) (Fig. 3, Panel A). This inhibitor had no effect on I $\kappa$ B $\alpha$  loss, a marker of canonical NF $\kappa$ B signalling (Fig. 3, Panel B), thus confirming the selectivity of SU1261 as a selective inhibitor of IKK $\alpha$ . As expected, SU1261 also concentration-dependently inhibited LIGHT induced p100 phosphorylation over a similar concentration range (Fig. 3, Panel C). In contrast, pre-incubation with the selective IKK $\beta$  inhibitor, IKK2-XI, had no effect on IL-1 $\beta$  induced pp100 phosphorylation (Fig. 3, Panel D), at concentrations which reversed cellular I $\kappa$ B $\alpha$  loss (Fig. 3, Panel E). Taken together these results strongly suggest a direct role for IKK $\alpha$  kinase activity in p100 phosphorylation in response to IL-1 $\beta$ .

It is well recognised that NIK has a central role in regulating p100 phosphorylation by facilitating the interaction of IKK $\alpha$  with p100 and promoting phosphorylation and subsequent processing. This was examined in Fig. 4 using the NIK inhibitor CW15337 [19]. As expected, the response to LIGHT was very susceptible to the inhibitor, a significant, almost complete reduction in p100 phosphorylation was observed at a concentration as low as 1  $\mu$ M (Fold increase: LIGHT + DMSO =  $8.421 \pm 1.492$  vs. 1  $\mu$ M =  $2.211 \pm 0.5021$ , \*\*\*P > 0.001) (Fig. 4, Panel A). This again was reflected in LIGHT-stimulated accumulation of cellular p52, which was reversed following CW15337 pre-treatment. Furthermore, LIGHT stimulated phosphorylation of p100 at the earliest time point of 60 min was completely abolished by pre-treatment with CW15337 at 5  $\mu$ M (Fig. 4, Panel B). Conversely over a similar

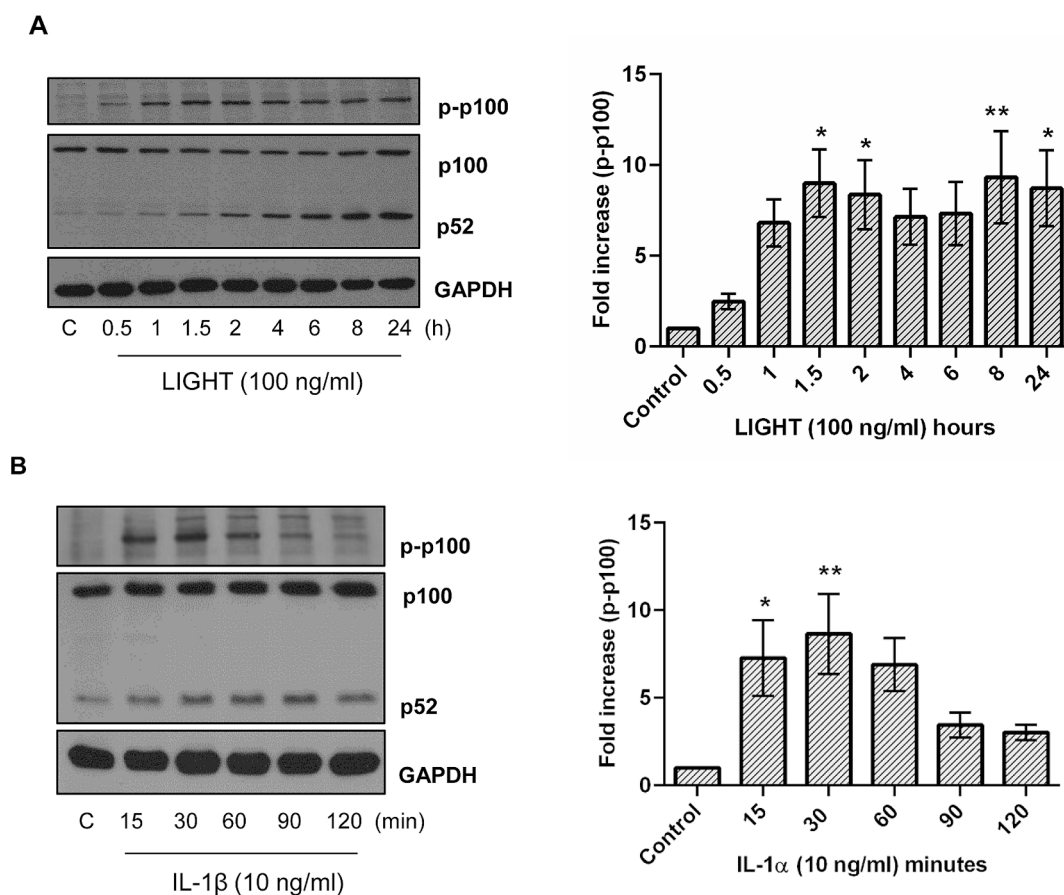


**Fig. 1.** IL-1 $\beta$  induces early activation of p100 phosphorylation in HUVECs. HUVECs were incubated with LIGHT (100 ng/ml, panel A) or IL-1 $\beta$  (10 ng/ml, Panel B) for the indicated time points. Whole cell lysates were assessed for pp100, p100/p52 and GAPDH as a loading control. Blots were semi-quantified using densitometry; results are representative of 4–5 independent experiments. \*P < 0.05, \*\*\*P < 0.001 relative to baseline control (c).

concentration range, CW15337 had little effect on IL-1 $\beta$  induced phosphorylation even up to concentrations as high as 20  $\mu$ M (Fold increase: IL-1 $\beta$  + DMSO = 13.05  $\pm$  3.550 vs. 20  $\mu$ M = 9.698  $\pm$  1.678) (Fig. 4, Panel C). In addition, CW15337 was without effect on IL-1 $\beta$  stimulation irrespective of the time point studies (including one co-incident with LIGHT stimulation at 60 min), demonstrating that IL-1 $\beta$  driven p100 phosphorylation was completely insensitive to NIK inhibition (Fig. 4, Panel D).

Having excluded NIK involvement in IL-1 $\beta$  –mediated p100 phosphorylation within the endothelial cells, we examined the potential for another MAP3K to play a role, namely TAK-1, as shown in Fig. 5. Pre-treatment with the TAK-1 inhibitor 5Z-7-Oxozealenol (5Z-7-oxo) [24], caused a concentration dependent inhibition of IL-1 $\beta$  induced p100 phosphorylation (Fold increase: IL-1 $\beta$  + DMSO = 6.125  $\pm$  1.456 vs. 5  $\mu$ M = 0.548  $\pm$  0.167, \*\*P > 0.01) (Fig. 5, Panel A). This inhibition was reflected at the level of IKK $\alpha$  activation; phosphorylation of IKK $\alpha$ , identified as the lower 85Kda band detected using a mixed ppIKK $\alpha$ /IKK $\beta$  phospho-antibody (serine 176/180), was again strongly inhibited at 5  $\mu$ M 5Z-7-oxo (Fold increase: IL-1 $\beta$  + DMSO = 22.21  $\pm$  4.264 vs. 1  $\mu$ M = 4.741  $\pm$  1.728, \*\*\*P > 0.001) (Fig. 5, Panel B). TAK-1 is recognised to be upstream of both the JNK and IKK $\beta$  –dependent canonical pathways [25] and indeed pre-treatment with 5Z-7-oxo also resulted in a concentration-dependent inhibition of IL-1 $\beta$  – mediated I $\kappa$ B $\alpha$  degradation (Fig. 5, Panel C) and JNK phosphorylation (Fold increase: IL-1 $\beta$  +

DMSO = 24.58  $\pm$  5.066 vs. 5  $\mu$ M = 2.723  $\pm$  0.9809, \*\*\*P > 0.001, Fig. 5, Panel D). These results support a role for TAK-1 in mediating the phosphorylation of p100 via activation of IKK $\alpha$ .

Having established the existence of a novel input into p100 phosphorylation in response to IL-1 $\beta$ , we examined the consequences for p52 translocation to the nucleus as indicated in Fig. 6. Again, to our surprise, IL-1 $\beta$  –stimulated a rapid increase in p52 nuclear translocation, peaking as early as 30 min (Fold increase: IL-1 $\beta$ , 30 min = 4.502  $\pm$  0.429, \*P < 0.05) (Fig. 6, Panel B). This contrasted with the slow, delayed increase in nuclear p52 accumulation in response to LIGHT which was apparent by 2 h and remained high over several hours (Fold increase: LIGHT, 4 h = 4.024  $\pm$  0.905, \*P < 0.05) (Fig. 6, Panel A). In addition, there was a marked difference in the nuclear accumulation of RelB. For LIGHT stimulation, translocation of RelB was, as expected, co-incident with p52. However, for IL-1 $\beta$  –stimulation nuclear translocation of RelB was delayed relative to p52, and only apparent after 60–90 min. This suggests that nuclear translocation of p52 mediated via IL-1 $\beta$  is not via the same mechanism as expected for standard non-canonical NF $\kappa$ B pathway activation.

Given such an early activation of p52 translocation we tested the contribution of NIK to IL-1 $\beta$  –induced p52 nuclear translocation (Fig. 7). However, again CW15337 had no significant effect upon IL-1 $\beta$  –stimulated p52 translocation at the early time points (Fold increase: IL-1 $\beta$  + DMSO = 4.713  $\pm$  1.699 vs. 10  $\mu$ M = 4.742  $\pm$  1.381) (Fig. 7, Panel

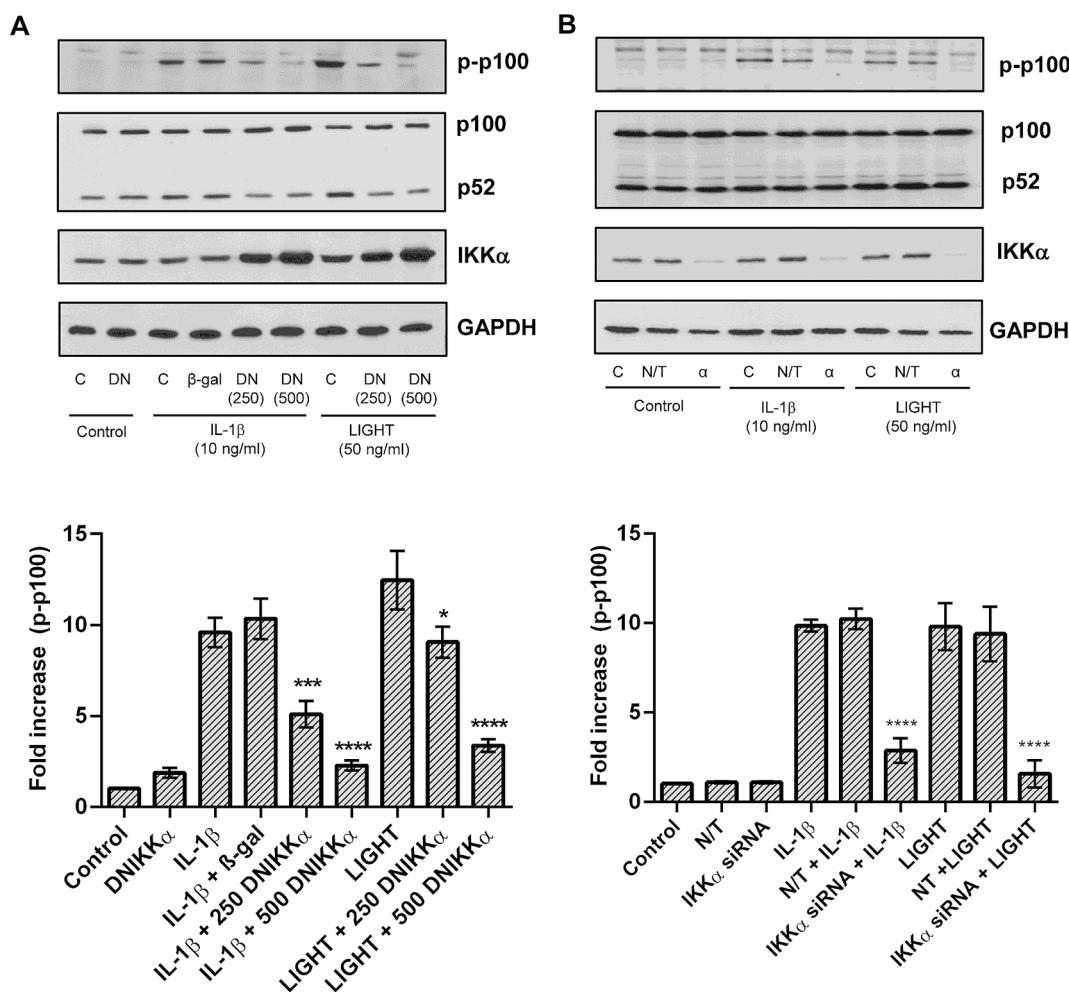


**Fig. 2.** Molecular inhibition of IKK $\alpha$  reduces IL-1 $\beta$  stimulated p100 phosphorylation in HUVECs In panel A, HUVECs were infected with increasing pfu of Adv. DN- IKK $\alpha$  or 500pfu of Adv. $\beta$  –gal for 40 h as indicated prior to stimulation with IL-1 $\beta$  (10 ng/ml) for 30 min or LIGHT (50 ng/ml) for 4 h. Alternatively, cells were incubated with 100 nM NT (non-targeted) or siRNA IKK $\alpha$  for 72 h (Panel B) prior to stimulation. Whole cell lysates were assessed as indicated for pp100, p100-52, IKK $\alpha$ , IKK $\beta$  and GAPDH as a loading control. Blots were semi-quantified using densitometry. Results are representative of at least 4 independent experiments. \*P < 0.05, \*\*P < 0.01, \*\*\*P < 0.001 compared with agonist-stimulated control.



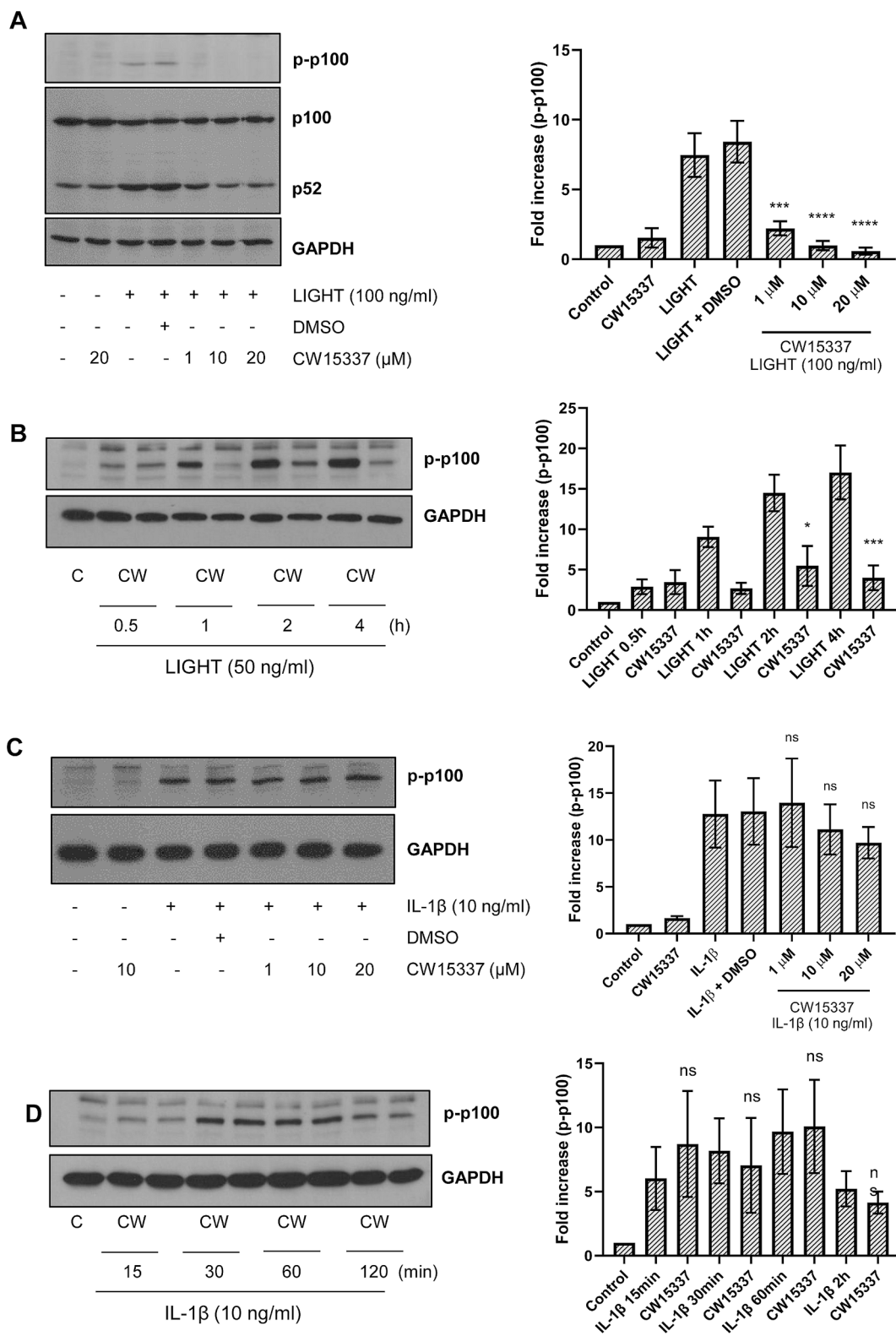


**Fig. 4.** Differential effect of NIK inhibitor CW15337 on IL-1 $\beta$  and LIGHT-induced p100 phosphorylation in HUVECs. HUVECs were pre-treated with CW15337 for 30 min prior to stimulation with LIGHT (100 ng/ml) for 30 min (Panel A) or IL-1 $\beta$  (10 ng/ml) for 4 h (Panel C) or pre-treated with 10  $\mu$ M CW15337 for 30 min prior to stimulation with LIGHT (50 ng/ml) or IL-1 $\beta$  (10 ng/ml) for the times indicated (Panel B & D). Whole cell lysates were assessed for pp100, p100/p52 with GAPDH as a loading control. Blots were semi-quantified using densitometry. Results are representative of at least 4 independent experiments. \*P < 0.05, \*\*P < 0.01, \*\*\*P < 0.001 compared with agonist-stimulated control.

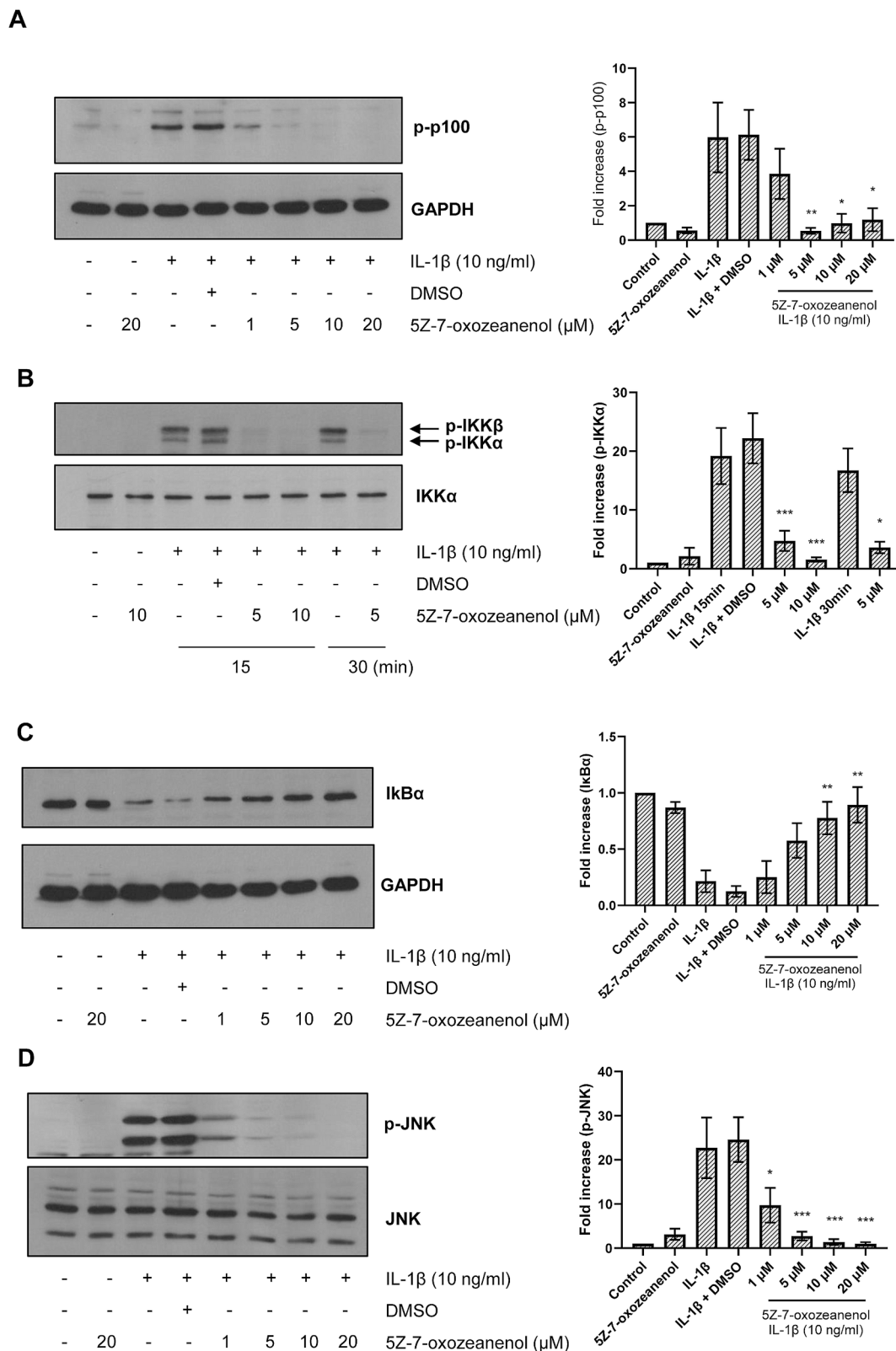


**Fig. 5.** TAK-1 inhibitor 5Z-7-oxozeanenol abrogates IL-1β – stimulated p100 and IKKα phosphorylation in HUVECs. HUVECs were pre-treated with increasing concentrations of 5Z-7-oxozeanenol for 60 min prior to stimulation with IL-1β (10 ng/ml) for a further 30 min. Whole cell lysates were assessed for pp100 (Panel A) or ppIKKα/β (Panel B), IκBα (Panel C), ppJNK (Panel D) or with total JNK, IKKα and/or GAPDH as a loading control. Blots were semi-quantified using densitometry. Results are representative of at least 4 independent experiments. \*P < 0.05, \*\*P < 0.01, \*\*\*P < 0.001 compared with agonist-stimulated control.

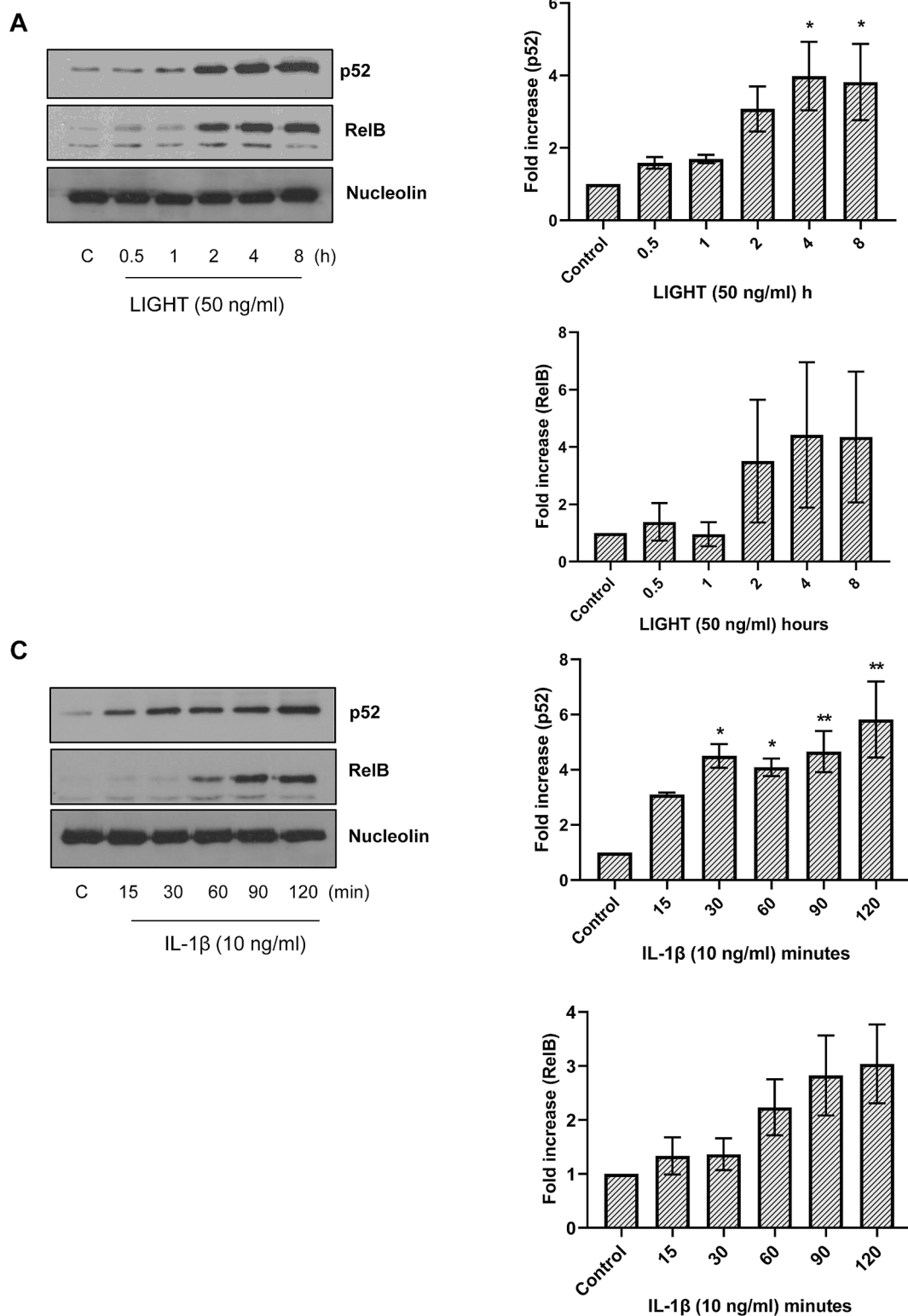


**Fig. 6.** IL-1 $\beta$  induces early nuclear translocation of p52 in HUVECs HUVECs were incubated with LIGHT (panel A) or IL-1 $\beta$  (Panel B) for the indicated time points. Nuclear extracts were assessed for p52 and RelB with nucleolin as a loading control. Blots were semi-quantified using densitometry; results are representative of 4–5 independent experiments. \*P < 0.05, \*\*P < 0.01 relative to baseline control.

5  $\mu$ M (Fold increase: (p52: IL-1 $\beta$  + DMSO = 4.373  $\pm$  0.537 vs. 5  $\mu$ M = 1.244  $\pm$  0.202, \*\*\*\*P > 0.0001), (p65: IL-1 $\beta$  + DMSO = 6.949  $\pm$  1.619 vs. 5  $\mu$ M = 1.904  $\pm$  0.697, \*P > 0.05) (Fig. 8, panel A). This suggested the potential for both NF $\kappa$ B pathways regulated by TAK-1 to regulate the nuclear translocation of p52.

The effect of IKK $\alpha$  inhibition on IL-1 $\beta$  –induced nuclear translocation of p52 and p65 was then examined as shown in Fig. 9. Pre-treatment of cells with Adv. DN-IKK $\alpha$  had a significant inhibitory effect on nuclear translocation of p52, reducing translocation by approximately 50 % (Fold increase: IL-1 $\beta$  +  $\beta$ -gal = 7.641  $\pm$  0.902 vs. 500 pfu = 2.431  $\pm$

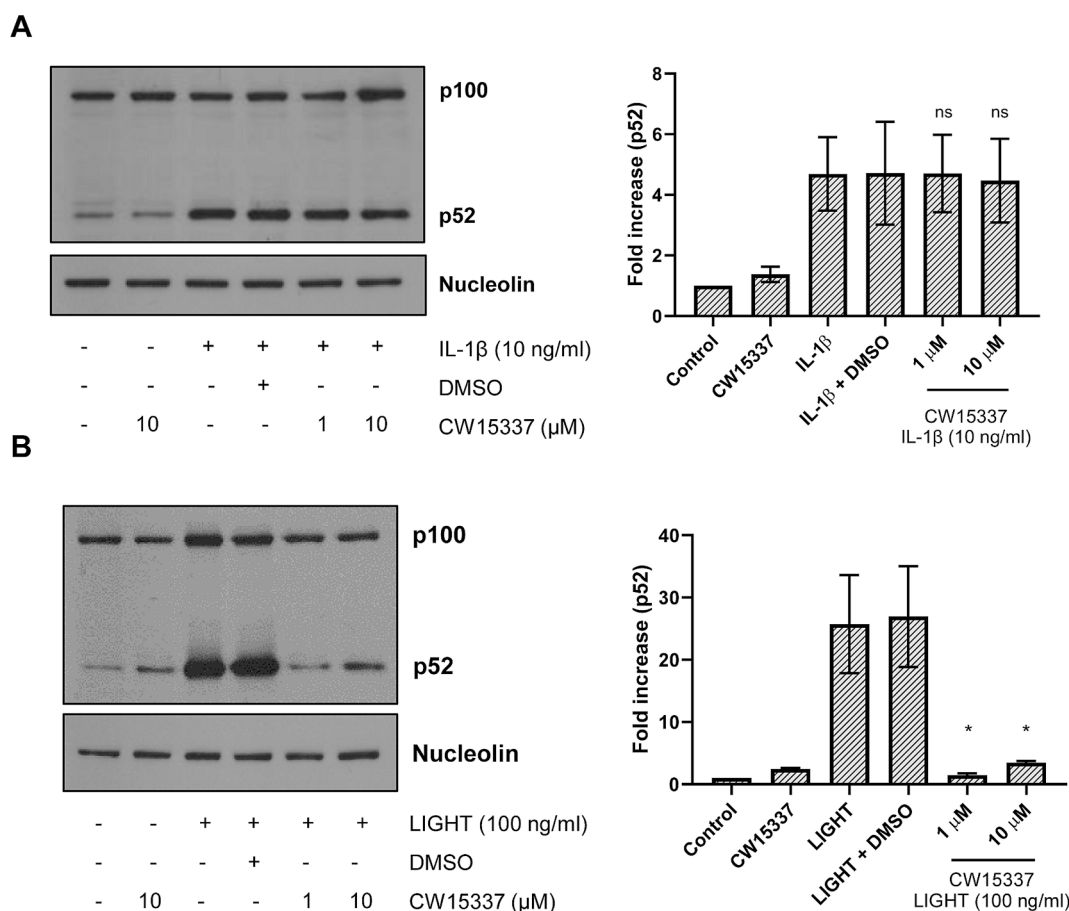


**Fig. 7.** Lack of effect of NIK inhibition on IL-1 $\beta$  – induced p52 nuclear translocation in HUVECs. HUVECs were pre-treated with CW15337 for 30 min prior to stimulation with 10 ng/ml of IL-1 $\beta$  for 30 min (Panel A) or 100 ng/ml LIGHT for 4 h (Panel B). Nuclear extracts were assessed for p100/p52, and nucleolin used as a loading control. Blots were semi-quantified using densitometry. The results are representative of at least 4 independent experiments. \* $P < 0.05$  compared with DMSO and agonist-stimulated control.

0.303, \* $P > 0.05$ ) (Fig. 9, Panel A). There was also a minor reduction in p65 translocation, although this inhibition did not reach significance. In addition, knockdown using IKK $\alpha$  siRNA significantly reduced p52 translocation, although again there was a partial reduction in p65 translocation, which did not reach significance (p52: N/T + IL-1 $\beta$  =  $4.478 \pm 0.649$  vs. IKK $\alpha$  siRNA + IL-1 $\beta$  =  $2.899 \pm 0.301$ , \* $P > 0.05$ ), (p65: N/T + IL-1 $\beta$  =  $4.869 \pm 0.417$  vs. IKK $\alpha$  siRNA + IL-1 $\beta$  =  $3.387 \pm 0.418$ ) (Fig. 9, Panel B). In contrast, pharmacological inhibition of IKK $\alpha$  using SU1261 resulted in a minor decrease in p52 nuclear translocation, which was not significant and there was no concomitant loss in p65 translocation (Fig. 9, Panel C). However, further experiments, shown in panel D, demonstrated that pre-treatment with SU1261 significantly reduced LIGHT induced nuclear translocation of p52 (p52: LIGHT + DMSO =  $8.297 \pm 2.320$ , vs. LIGHT + 1  $\mu$ M SU1261  $2.847 \pm 0.9855n = 4$ ,  $p < 0.005$ ) confirming that SU1261 is effective in inhibiting IKK $\alpha$  – mediated p100 processing as part of the non-canonical NF $\kappa$ B pathway.

Inhibition of IKK $\beta$  was found to be more effective compared to IKK $\alpha$  with respect to p52 nuclear translocation as shown in Fig. 10. Infection with an Adv-DN-IKK $\beta$  strongly inhibited both p52 and p65 translocation reducing translocation to near basal levels at 50 and 100 pfu (Fold increase: (p52: IL-1 $\beta$  +  $\beta$ -gal =  $8.014 \pm 0.789$  vs. 50 pfu =  $2.328 \pm 0.593$ , \*\*\* $P > 0.001$ ), (p65: IL-1 $\beta$  +  $\beta$ -gal =  $7.911 \pm 1.305$  vs. 50 pfu =  $2.642 \pm 0.236$ , \*\*\* $P > 0.001$ )) (Fig. 10, Panel A). Simultaneous experiments confirmed inhibition of the canonical NF $\kappa$ B pathway via complete reversal of IL-1 $\beta$  – induced cellular I $\kappa$ B $\alpha$  loss (Fig. 10, Panel B). In addition, in cells preincubated with the IKK2-X1 inhibitor, – a significant concomitant reduction in both p52 and p65 translocation at 10 and

30  $\mu$ M was observed (Fig. 10, panel C). This corresponds with concentrations that reverse cellular I $\kappa$ B $\alpha$  loss (Fold increase: (p52: IL-1 $\beta$  + DMSO =  $16.655 \pm 4.872$  vs. 30  $\mu$ M =  $4.798 \pm 1.936$ , \*\*\* $P > 0.001$ ), (p65: IL-1 $\beta$  + DMSO =  $12.896 \pm 1.926$  vs. 30  $\mu$ M =  $4.782 \pm 1.632$ , \* $P > 0.05$ )) (see Fig. 3, panel E). Taken together these results suggest a significant role for the canonical NF $\kappa$ B pathway in the translocation of p52 to the nucleus in response to IL-1 $\beta$ .

#### 4. Discussion

In this study we have identified two new novel mechanisms with respect to the activation of the non-canonical NF $\kappa$ B pathway and nuclear p52 translocation stimulated by IL-1 $\beta$  in endothelial cells. Initially, we identified a novel early activation of p100 phosphorylation in response to IL-1 $\beta$  distinct from the more delayed phosphorylation of p100 by LIGHT. Whilst in the majority of studies to date, phosphorylation of p100 has not been routinely assessed, this event is recognised as bona-fide mechanism within the non-canonical NF $\kappa$ B pathway stimulated by classical non-canonical ligands such as LT $\alpha$ 1 $\beta$ 2, LIGHT and CD40L [4,6]. Our studies show that IL-1 $\beta$  stimulation can also result in phosphorylation of this key marker in endothelial cells and is consistent with a recent study using a bone cancer cell line [26]. More common is the measurement of the delayed accumulation of cellular p52, which in our study, in response to LIGHT, compares favourably with previous studies in endothelial cells stimulated with either LIGHT, LT $\alpha$ 1 $\beta$ 2 [12,15,16] or CD40 ligand [13] suggesting the non-canonical NF $\kappa$ B pathway is fully activated in this cell type. Significantly, IL-1 $\beta$  did not cause any

A

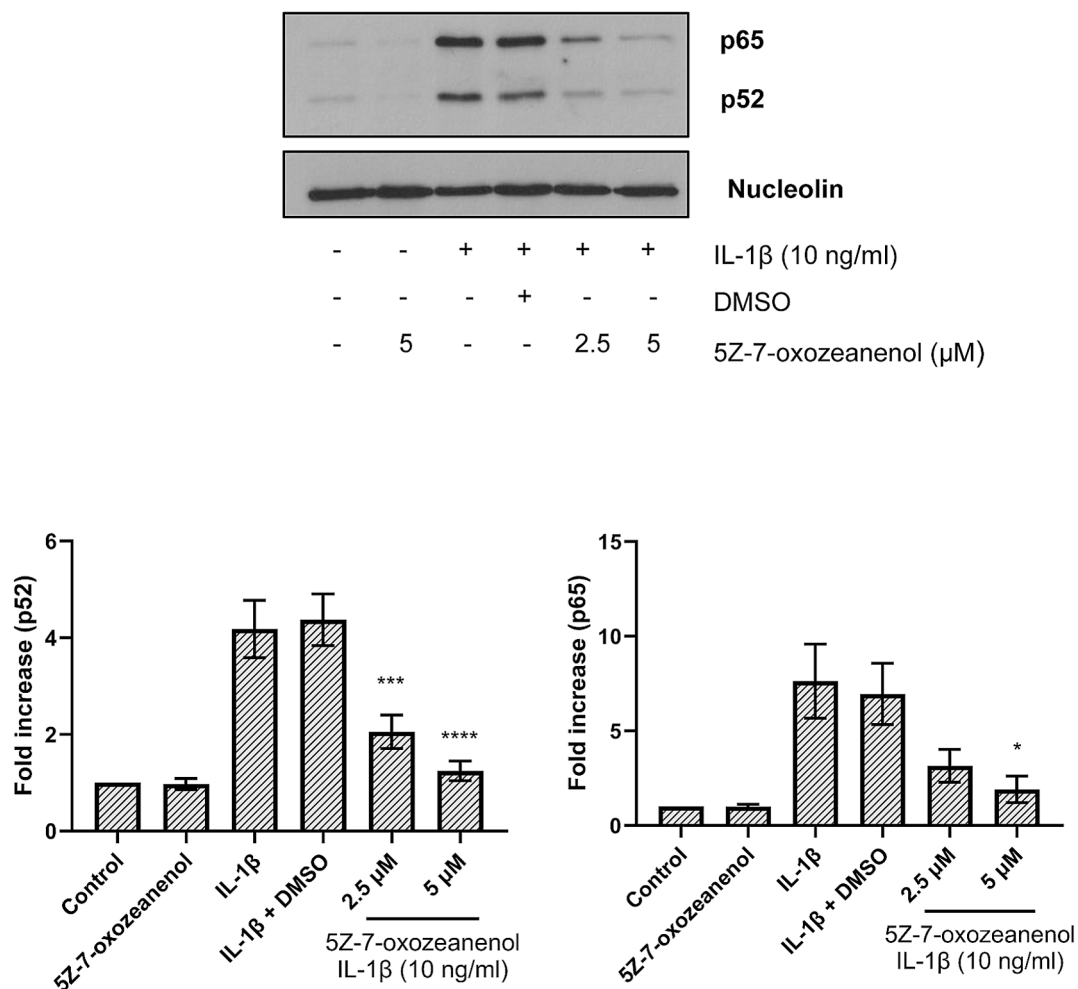


**Fig. 8.** Inhibition of TAK-1 reduces IL-1 $\beta$  – induced p52 and p65 nuclear translocation in HUVECs. HUVECs were pre-treated with 2.5 and 5  $\mu$ M 5Z-7-oxozeanenol for 60 min as indicated prior to stimulation with IL-1 $\beta$  (10 ng/ml) for 30 min. Nuclear extracts were simultaneously assessed for p52 and p65 and nucleolin used as a loading control. Blots were semi-quantified using densitometry. The results are representative of at least 4 independent experiments. \* $P < 0.05$ , \*\*\* $P < 0.001$ , \*\*\*\* $P < 0.0001$  compared with agonist-stimulated control.

accumulation of cellular p52 or concomitant loss in p100 suggesting a divergence downstream within the pathway.

It is well recognised that IKK $\alpha$  plays a central role in the phosphorylation of p100 in response to non-canonical ligands; deletion of the protein significantly inhibits pathway activation [7,8]. In this study, selective interventions through DN-IKK $\alpha$ , IKK $\alpha$  siRNA or a novel first-in-class selective IKK $\alpha$  inhibitor SU1261 caused significant inhibition of p100 phosphorylation by IL-1 $\beta$ , confirming the role of IKK $\alpha$  in this novel axis. A previous *in vitro* study, using transfected IKK $\alpha$  and mutated p100 isoforms, indicated catalytic activity of IKK $\alpha$  was not necessarily required to mediate serine 866/870 phosphorylation suggestive of another kinase which plays this role [7,8]. Our experiments using the novel selective IKK $\alpha$  inhibitor, SU1261, an ATP binding site inhibitor, confirms that the kinase activity of IKK $\alpha$  is essential for phosphorylation of p100 within these residues. Experiments also used IKK $\alpha$  siRNA as shown previously [15], however this approach requires some caution in interpretation as deletion of a single component of the NEMO/IKK $\alpha$ / $\beta$  complex can result in disruption and lack of function [27]. Nevertheless, a clear loss in p100 phosphorylation was also recorded, again comparable with a recent study in U2OS cells employing IKK $\alpha$  CRISPR deletion [26].

Further elucidation of a novel pathway was found using a recently

described NIK inhibitor, CW15337 [19]. A number of putative NIK inhibitors have been used previously [28–30], however these have not been assessed appropriately for their ability to inhibit non-canonical NF $\kappa$ B signalling. Recently, CW15337 has been shown to inhibit CD40L-induced p52 formation in chronic lymphocytic leukaemia cells [19]. We have extended those observations to show that stimulation of p100 phosphorylation and cellular accumulation of p52 stimulated by LIGHT ligand is abolished following NIK inhibitor treatment, consistent with a previous study in endothelial cells using a different NIK inhibitor [31], or where NIK has been silenced [15]. This accords with the general model originally defined in a number of early studies; NIK is essential to bring IKK $\alpha$  into a complex with p100 to mediate phosphorylation and additionally, promotes the binding of p100 to the beta-transducin repeats-containing proteins ( $\beta$ -TrCP) E3 ubiquitin ligase to activate processing [6–8]. It also confirms the validity of the inhibitory approach and confirms the involvement of a NIK-dependent mechanism in conventional non-canonical NF $\kappa$ B signalling in endothelial cells.

However, our finding that IL-1 $\beta$  –induced p100 phosphorylation independent of NIK suggests an alternative route to p100 activation, which does not require NIK to bring IKK $\alpha$  into proximity with p100 to mediate phosphorylation; the stabilisation of NIK required for activation of the non-canonical pathway in endothelial cells is unlikely to have

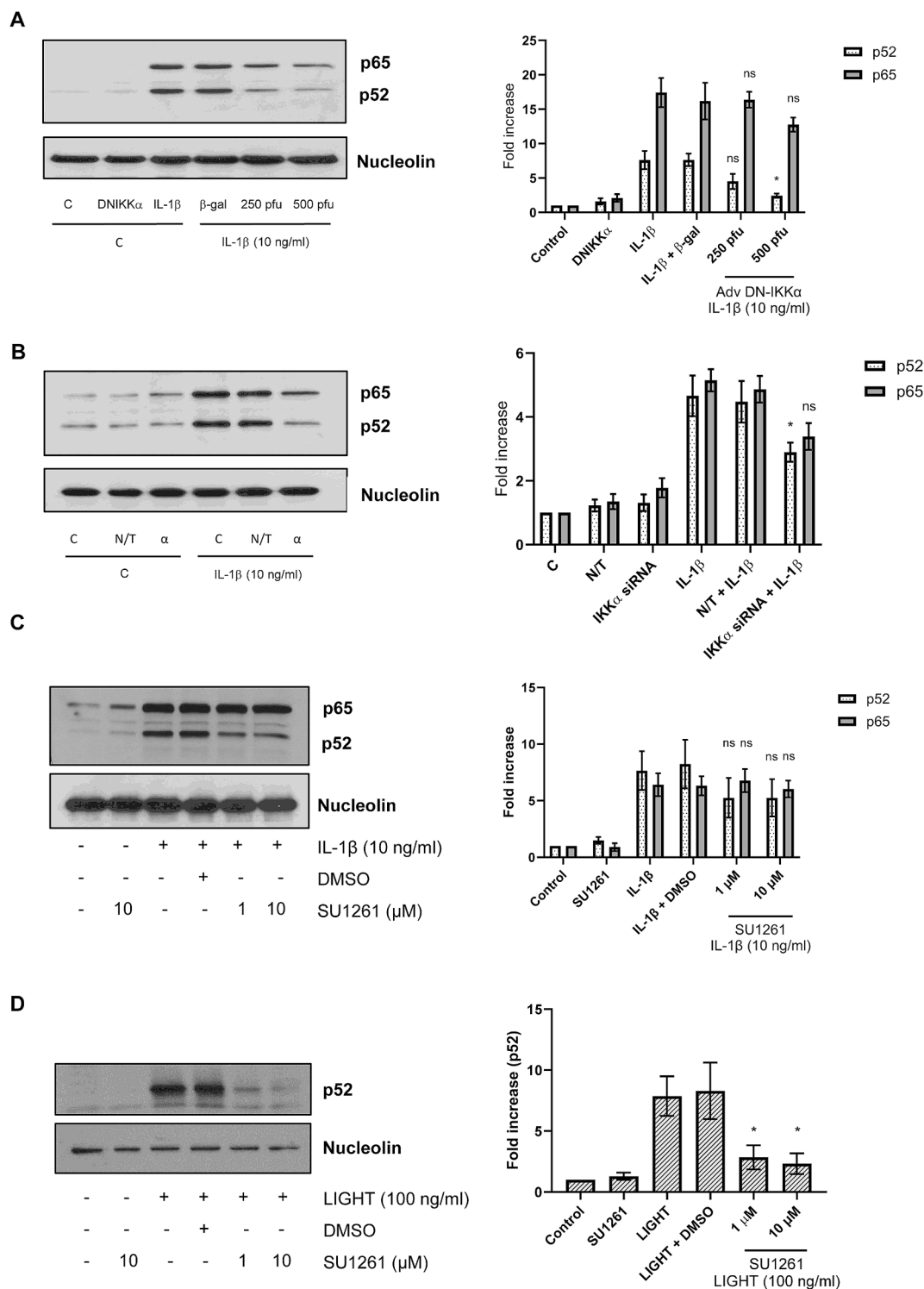


**Fig. 9.** Effect of IKKα inhibition on IL-1β – induced p52/p65 nuclear translocation in HUVECs. HUVECs were infected with 250 and 500 pfu of Adv DN-IKKα or 500 pfu of Adv.β – gal for 40 h (Panel A), transfected with 100 nM N/T and IKKα siRNA for 72 h (Panel B) or varying concentrations of SU1261 (Panels C & D) for 30 min prior to stimulation with IL-1β (10 ng/ml) for a further 30 min (Panels A-C), or LIGHT for a further 4 h (Panel D). Nuclear extracts were assessed simultaneously for p52 and p65 with nucleolin used as loading control. The results are representative of at least 4 independent experiments. Blots were semi-quantified using densitometry. \*P < 0.05 compared with agonist-stimulated control.

occurred in such a short period of time. Therefore, another intermediate may play a role in facilitating the binding of IKKα to p100 following IL-1β stimulation. We found for the first time in endothelial cells, that TAK-1 could regulate phosphorylation of p100 and therefore could also play a role in facilitating IKKα binding to p100. However, we also show that TAK-1, which is recognised to be upstream of the NEMO/IKKα/β

complex also regulates IKKα phosphorylation, working further upstream within the cascade as suggested in a number of studies [32,33]. This suggests that IKKα phosphorylation of p100 by IL-1β stimulation may emanate from the canonical NEMO/IKKα/β complex, and that another intermediate may still be required to facilitate binding of IKKα to p100 in the absence of NIK. TAK-1 has been shown to be strongly expressed in

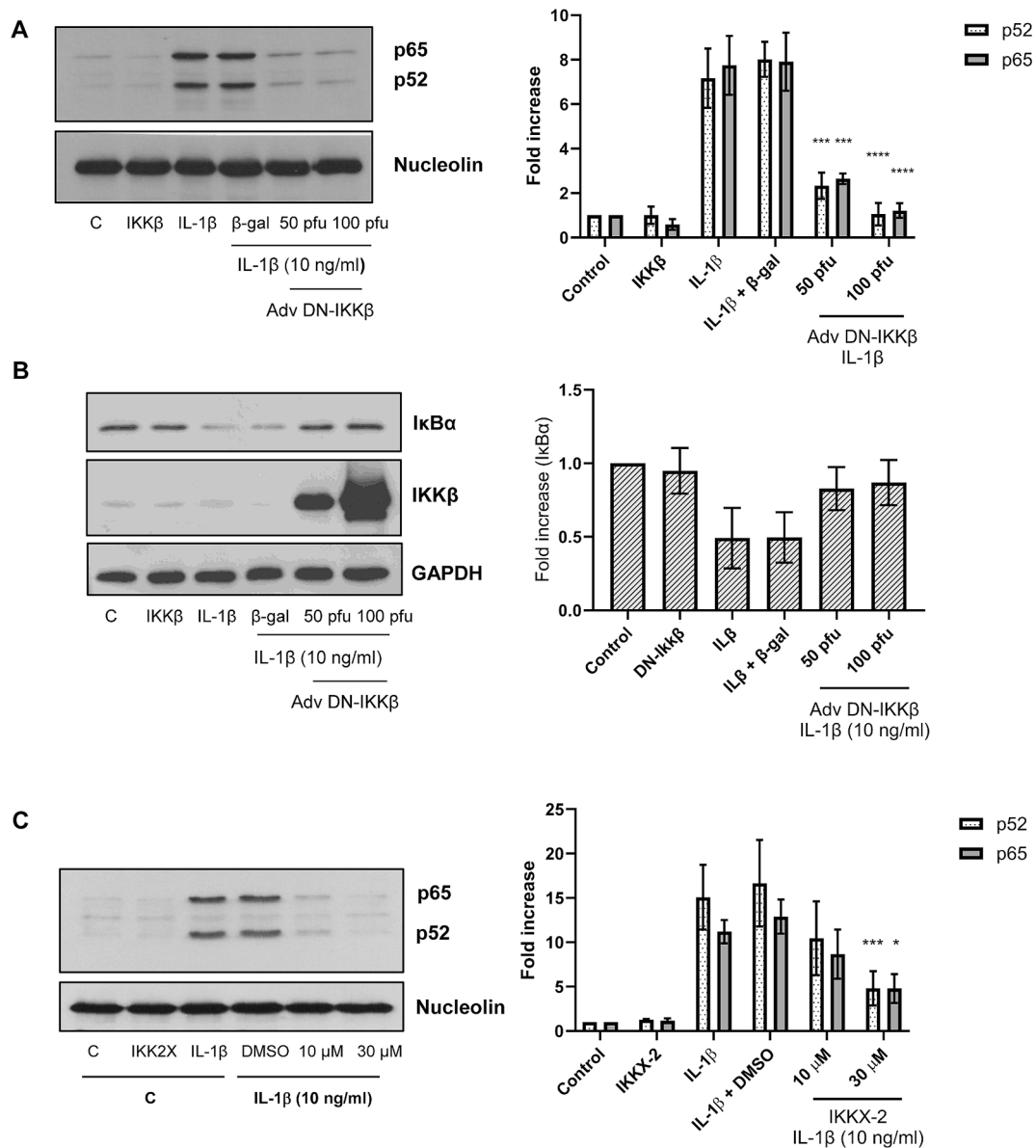


**Fig. 10.** Inhibition of IKK $\beta$  abrogates IL-1 $\beta$  – induced p52 nuclear translocation in HUVECs. HUVECs were infected with 50 and 100 pfu of Adv DN-IKK $\beta$  or 100pfu of Adv. $\beta$  –gal (Panels A and B) for 40 h or IKK2-X1 (Panel C) for 30 min prior to stimulation with IL-1 $\beta$  (10 ng/ml) for a further 30 min. Samples were assessed simultaneously for nuclear p52 and p65 (Panels A & C), or I $\kappa$ B $\alpha$  levels (Panel B) with nucleolin or GAPDH as loading control. Blots were semi-quantified using densitometry. The results are representative of at least 4 independent experiments. \*P < 0.05, \*\*\*P < 0.001, \*\*\*\*P < 0.0001 compared with agonist-stimulated control.

the endothelium and shown to mediate cell survival [34,35]. Our findings further expand the function of TAK-1 with respect to this novel axis in endothelial cells.

In this study we have also identified another novel feature of the cascade: IL-1 $\beta$  stimulated a rapid increase in the nuclear translocation of p52. Such a finding has not been previously identified with respect to p52, the current model suggests that non-canonical NF $\kappa$ B signalling, results in the NIK-induced processing of p100 such that p52 once formed will translocate usually as a p52/RelB dimer to the nucleus [36]. We found that the kinetics of nuclear translocation for p52 and RelB were dissociated following IL-1 $\beta$  stimulation. Nuclear RelB was not found to be enhanced until 60 min at the earliest, presumably dependent on RelA-mediated induction of RelB [37], suggesting a different mechanism of regulation. Secondly, we found that NIK inhibition was without effect on p52 translocation, suggesting that p52 does not derive from p100 processing in this scenario. We posit that p52 comes from an existing

cytosolic pool and is translocated due to the presence of an nuclear localisation sequence in the C-terminus of p52 which is revealed following agonist stimulation [38].

Additional experiments sought to determine the relationship between p100 phosphorylation and p52 translocation downstream of TAK-1. A number of studies [39–41] have indicated the presence of a multimeric p100 complex in the cytosol as part of a NF $\kappa$ Bosome [41]. This complex is able to sequester a number of NF $\kappa$ B subunits including p52. Such a pool is thought to be distinct from the p100 involved in processing [42]. Thus, IL-1 $\beta$  –mediated p100 phosphorylation within an existing pool of p100 bound to p52 may then promote dissociation of p52 and nuclear translocation.

Our studies did not support a strong link between the two events. Whilst DN-IKK $\alpha$  and siRNA IKK $\alpha$  did result in some loss in p52 translocation, it also resulted in the partial inhibition of p65 translocation. Indeed, we found that pharmacological inhibition of IKK $\alpha$  alone had no

significant effect on p52 translocation. However, we also demonstrate that IKK $\beta$  inhibition itself, abolished both IL-1 $\beta$  induced p52 and p65 nuclear translocation. This suggests that particularly siRNA IKK $\alpha$  may have an indirect effect upon IKK $\beta$  activity due to disruption of the NEMO/IKK $\beta$  /IKK $\alpha$  complex and it is IKK $\beta$  /p65 that drives the nuclear translocation of p52. Indeed, Cook and colleagues have shown that CRISPR-induced loss of IKK $\alpha$  results in an abrogation of p65 nuclear translocation [43], thus we suggest a reciprocal effect; loss of IKK $\alpha$  reduces p65 translocation which, in-turn, reduces p52 translocation. Thus, p52 which normally forms p52/RelB dimers could rapidly translocate to the nucleus as a homodimer or as a p65/p52 dimer. Recent studies have demonstrated the formation of latent RelA/p52 dimers in infection [44,45], suggesting such a complex can be formed following appropriate cell stimulation.

In conclusion, we have uncovered two novel aspects of NF $\kappa$ B regulation mediated via IL-1 $\beta$  in endothelial cells, which have not been previously explored. Further studies are needed to link the phosphorylation of p100 and p52 nuclear translocation with gene regulation stimulated in response to IL-1 $\beta$ . For example, p52 homodimers can, in conjunction with Bcl3 [46], function as both positive and negative regulators of gene transcription [36,47] and it remains to be determined how this complex regulates gene promoter activity in endothelial cells. Given the challenges with using siRNA or CRISPR in primary cell types, the development of SU1261 and other novel IKK $\alpha$  compounds represent a crucial step forward in defining the role of IKK $\alpha$  in cells and its potential to be therapeutically targeted.

#### CRedit authorship contribution statement

**Rachel Craig:** Investigation, Formal analysis, Data curation. **Kathryn McIntosh:** Writing – review & editing, Writing – original draft, Visualization, Validation, Supervision, Software, Resources, Project administration, Methodology, Investigation, Funding acquisition, Formal analysis, Data curation, Conceptualization. **Ka Ho Ho:** Data curation. **Ashley McCulloch:** Data curation. **Christopher Riley:** Resources. **Christopher Lawson:** Resources. **Simon P. Mackay:** Resources. **Andrew Paul:** Writing – review & editing, Resources, Methodology, Funding acquisition, Conceptualization. **Paul Coats:** Funding acquisition. **Robin Plevin:** Writing – original draft, Visualization, Supervision, Resources, Project administration, Investigation, Funding acquisition, Data curation, Conceptualization.

#### Declaration of competing interest

The authors declare that they have no known competing financial interests or personal relationships that could have appeared to influence the work reported in this paper.

#### Acknowledgements

This work was sponsored by a BHF studentship (FS/18/36/33686).

#### Data availability

Data will be made available on request.

#### References

- J.A. Prescott, J.P. Mitchell, S.J. Cook, Inhibitory feedback control of NF-kappaB signalling in health and disease, *Biochem J* 478 (13) (2021) 2619–2664.
- C. Gamble, et al., Inhibitory kappa B Kinases as targets for pharmacological regulation, *Br J Pharmacol* 165 (4) (2012) 802–819.
- S.C. Sun, The noncanonical NF-kappaB pathway, *Immunol Rev* 246 (1) (2012) 125–140.
- S.C. Sun, The non-canonical NF-kappaB pathway in immunity and inflammation, *Nat Rev Immunol* 17 (9) (2017) 545–558.
- C. Dostert, et al., The TNF Family of Ligands and Receptors: Communication Modules in the Immune System and Beyond, *Physiol Rev* 99 (1) (2019) 115–160.
- C. Liang, M. Zhang, S.C. Sun, beta-TrCP binding and processing of NF-kappaB2/p100 involve its phosphorylation at serines 866 and 870, *Cell Signal* 18 (8) (2006) 1309–1317.
- G. Xiao, A. Fong, S.C. Sun, Induction of p100 processing by NF-kappaB-inducing kinase involves docking IkkappaB kinase alpha (IKKalpha) to p100 and IKKalpha-mediated phosphorylation, *J Biol Chem* 279 (29) (2004) 30099–30105.
- G. Xiao, E.W. Harhaj, S.C. Sun, NF-kappaB-inducing kinase regulates the processing of NF-kappaB2 p100, *Mol Cell* 7 (2) (2001) 401–409.
- G. Liao, et al., Regulation of the NF-kappaB-inducing kinase by tumor necrosis factor receptor-associated factor 3-induced degradation, *J Biol Chem* 279 (25) (2004) 26243–26250.
- S. Vallabhapurapu, et al., Nonredundant and complementary functions of TRAF2 and TRAF3 in a ubiquitination cascade that activates NIK-dependent alternative NF-kappaB signaling, *Nat Immunol* 9 (12) (2008) 1364–1370.
- B.J. Zarnegar, et al., Noncanonical NF-kappaB activation requires coordinated assembly of a regulatory complex of the adaptors cIAP1, cIAP2, TRAF2 and TRAF3 and the kinase NIK, *Nat Immunol* 9 (12) (2008) 1371–1378.
- L.A. Madge, et al., Lymphotoxin-alpha 1 beta 2 and LIGHT induce classical and noncanonical NF-kappa B-dependent proinflammatory gene expression in vascular endothelial cells, *J Immunol* 180 (5) (2008) 3467–3477.
- J. Seigner, et al., CD40L and TNF both activate the classical NF-kappaB pathway, which is not required for the CD40L induced alternative pathway in endothelial cells, *Biochem Biophys Res Commun* 495 (1) (2018) 1389–1394.
- E. Harper, et al., Activation of the non-canonical NF-kappaB/p52 pathway in vascular endothelial cells by RANKL elicits pro-calcific signalling in co-cultured smooth muscle cells, *Cell Signal* 47 (2018) 142–150.
- P. Kucharzewska, et al., NIK-IKK complex interaction controls NF-kappaB-dependent inflammatory activation of endothelium in response to LTbetaR ligation, *J Cell Sci* 132 (7) (2019).
- L.A. Madge, M.J. May, Classical NF-kappaB activation negatively regulates noncanonical NF-kappaB-dependent CXCL12 expression, *J Biol Chem* 285 (49) (2010) 38069–38077.
- C.M. Gray, et al., Noncanonical NF-kappaB signaling is limited by classical NF-kappaB activity, *Sci Signal* 7 (311) (2014) p. ra13.
- A. Paul, et al., Inhibitory-kappaB Kinase (IKK) alpha and Nuclear Factor-kappaB (NFkappaB)-Inducing Kinase (NIK) as Anti-Cancer Drug Targets, *Cells* 7 (10) (2018).
- M. Haselager, et al., Regulation of Bcl-XL by non-canonical NF-kappaB in the context of CD40-induced drug resistance in CLL, *Cell Death Differ* 28 (5) (2021) 1658–1668.
- C.J. MacKenzie, et al., IKKalpha and IKKbeta function in TNFalpha-stimulated adhesion molecule expression in human aortic smooth muscle cells, *Cell Signal* 19 (1) (2007) 75–80.
- C.J. MacKenzie, et al., Enhancement of lipopolysaccharide-stimulated JNK activity in rat aortic smooth muscle cells by pharmacological and adenovirus-mediated inhibition of inhibitory kappa B kinase signalling, *Br J Pharmacol* 139 (5) (2003) 1041–1049.
- N.G. Anthony, et al., Inhibitory Kappa B Kinase alpha (IKKalpha) Inhibitors That Recapitulate Their Selectivity in Cells against Isoform-Related Biomarkers, *J Med Chem* 60 (16) (2017) 7043–7066.
- C. Riley, et al., Design and Synthesis of Novel Aminooindazole-pyrrolo[2,3-b]pyridine Inhibitors of IKKalpha That Selectively Perturb Cellular Non-Canonical NF-kappaB Signalling, *Molecules* 29 (15) (2024).
- J. Wu, et al., Mechanism and in vitro pharmacology of TAK1 inhibition by (5Z)-7-Oxozeanol, *ACS Chem Biol* 8 (3) (2013) 643–650.
- S. Sato, et al., Essential function for the kinase TAK1 in innate and adaptive immune responses, *Nat Immunol* 6 (11) (2005) 1087–1095.
- K. McIntosh, et al., IL-1beta stimulates a novel, IKKalpha -dependent, NIK -independent activation of non-canonical NFkappaB signalling, *Cell Signal* 107 (2023) 110684.
- O. Sokolova, G. Maubach, M. Naumann, MEK3 and TAK1 synergize to activate IKK complex in Helicobacter pylori infection, *Biochim Biophys Acta* 1843 (4) (2014) 715–724.
- Y.N. Demchenko, et al., Novel inhibitors are cytotoxic for myeloma cells with NFkB inducing kinase-dependent activation of NFkB, *Oncotarget* 5 (12) (2014) 4554–4566.
- J. Mortier, et al., NF-kappaB inducing kinase (NIK) inhibitors: identification of new scaffolds using virtual screening, *Bioorg Med Chem Lett* 20 (15) (2010) 4515–4520.
- X. Ren, et al., A small-molecule inhibitor of NF-kappaB-inducing kinase (NIK) protects liver from toxin-induced inflammation, oxidative stress, and injury, *FASEB J* 31 (2) (2017) 711–718.
- C.X. Maracle, et al., Targeting non-canonical nuclear factor-kappaB signalling attenuates neovascularization in a novel 3D model of rheumatoid arthritis synovial angiogenesis, *Rheumatology (oxford)* 56 (2) (2017) 294–302.
- M. Blonska, et al., TAK1 is recruited to the tumor necrosis factor-alpha (TNF-alpha) receptor 1 complex in a receptor-interacting protein (RIP)-dependent manner and cooperates with MEK3 leading to NF-kappaB activation, *J Biol Chem* 280 (52) (2005) 43056–43063.
- J. Yao, et al., Interleukin-1 (IL-1)-induced TAK1-dependent Versus MEK3-dependent NFkappaB activation pathways bifurcate at IL-1 receptor-associated kinase modification, *J Biol Chem* 282 (9) (2007) 6075–6089.
- H. Naito, et al., TAK1 Prevents Endothelial Apoptosis and Maintains Vascular Integrity, *Dev Cell* 48 (2) (2019) 151–166 e7.
- H. Naito, N. Takakura, TAK1 safeguards endothelial cells from gut microbes and inflammation, *Mol Cell Oncol* 6 (3) (2019) 1588657.

- [36] G. Ghosh, V.Y. Wang, Origin of the Functional Distinctiveness of NF-kappaB/p52, *Front Cell Dev Biol* 9 (2021) 764164.
- [37] S. Basak, V.F. Shih, A. Hoffmann, Generation and activation of multiple dimeric transcription factors within the NF-kappaB signaling system, *Mol Cell Biol* 28 (10) (2008) 3139–3150.
- [38] R. Fagerlund, et al., NF-kappaB p52, RelB and c-Rel are transported into the nucleus via a subset of importin alpha molecules, *Cell Signal* 20 (8) (2008) 1442–1451.
- [39] S. Basak, et al., A fourth IkappaB protein within the NF-kappaB signaling module, *Cell* 128 (2) (2007) 369–381.
- [40] O.V. Savinova, A. Hoffmann, G. Ghosh, The Nfkb1 and Nfkb2 proteins p105 and p100 function as the core of high-molecular-weight heterogeneous complexes, *Mol Cell* 34 (5) (2009) 591–602.
- [41] Z. Tao, et al., p100/IkappaBdelta sequesters and inhibits NF-kappaB through kappaBsome formation, *Proc Natl Acad Sci U S A* 111 (45) (2014) 15946–15951.
- [42] Z.B. Yilmaz, et al., Quantitative dissection and modeling of the NF-kappaB p100–p105 module reveals interdependent precursor proteolysis, *Cell Rep* 9 (5) (2014) 1756–1769.
- [43] J.A. Prescott, et al., IKKalpha plays a major role in canonical NF-kappaB signalling in colorectal cells, *Biochem J* 479 (3) (2022) 305–325.
- [44] B. Banoth, et al., Stimulus-selective crosstalk via the NF-kappaB signaling system reinforces innate immune response to alleviate gut infection, *Elife* 4 (2015).
- [45] M. Chawla, et al., An epithelial Nfkb2 pathway exacerbates intestinal inflammation by supplementing latent RelA dimers to the canonical NF-kappaB module, *Proc Natl Acad Sci U S A* 118 (25) (2021).
- [46] W. Pan, et al., Atypical IkappaB Bcl3 enhances the generation of the NF-kappaB p52 homodimer, *Front Cell Dev Biol* 10 (2022) 930619.
- [47] V.Y. Wang, et al., The transcriptional specificity of NF-kappaB dimers is coded within the kappaB DNA response elements, *Cell Rep* 2 (4) (2012) 824–839.